

Amphibole.

Amphibole is a scarce mineral in the rocks from the Esquinzo ultra-alkaline Complex. It only occurs in perovskite-bearing amphibole pyroxenites from las Montañetas and amphibole pyroxenites-melteigites from Playa de Tebeto.

Amphibole crystals in perovskite-bearing amphibole pyroxenites from las Montañetas are classified as Mg-hastingsite/pargasite. They have high Ti content (2.86-4.22 wt% TiO₂, Ti: 0.32-0.48 a.p.f.u., Table S6 and Figure S8; Mg/Mg+Fe²⁺-Ti diagram), but not high enough to classify these amphiboles as kaersutites. Probably this is caused by simultaneous crystallization of abundant perovskite, that takes large amounts of Ti from magma.

In amphibole-bearing melteigites from Playa de Tebeto, red cores are kaersutites. Red rims have a pargasite/Mg-hastingsite composition while green rims have a ferropargasite/hastingsite composition (Figure S8: Mg/Mg+Fe²⁺-Si, Mg/Mg+Fe²⁺-K and Mg/Mg+Fe²⁺-Mn diagrams). In this zoning scheme, Si, K and Mn increase while Mg/Mg+Fe²⁺ ratio decrease (Figure S8, Mg/Mg+Fe²⁺-Ti diagram) that correlates with the crystallization of an ultra-alkaline magma. Amphiboles in pyroxenite xenoliths or as xenocrysts in the rocks of the Submarine Volcanic Group are kaersutites [25].

Titanite-

Titanite is an accessory mineral in all rock types from the Esquinzo ultra-alkaline Complex. In the less differentiated rocks (pyroxenites, melteigites and ijolites), titanite is close to the ideal formula: Ca Ti (SiO₄) (O, OH, F). Nevertheless, titanites in pegmatite ijolites from Las Montañetas and malignites from Playa del Águila have moderate Nb₂O₅, ZrO₂ and REE contents (Table S7). Nb₂O₅ contents reach 0.31 wt%. ZrO₂ contents are up to 0.45 wt% in malignites from Playa del Águila, although in pegmatite ijolites from Las Montañetas, ZrO₂ reaches 2.05 wt%.

REE contents are always moderate with Ce₂O₃ around 0.25 wt% in titanites in ijolite pegmatite from Las Montañetas. Titanites from Playa del Águila malignites show a marked compositional zoning with an increase in Ce₂O₃ contents from core (0.02 wt%) to rim (0.39 wt%).

Titanite can incorporate Nb, Ta, REE, Zr and Na in its structure [77]. The chemical variations in the titanite of the Esquinzo ultra-alkaline complex are controlled through the following substitution mechanisms (Table S7 and Figure S9):

- a) $\text{Ca}^{2+} + \text{Ti}^{4+} \rightleftharpoons \text{REE}^{3+} + (\text{Al}, \text{Fe}^{3+})$
- b) $2\text{Ti}^{4+} \rightleftharpoons \text{Nb}^{5+} + (\text{Al}, \text{Fe}^{3+})$
- c) $\text{Ti}^{4+} \rightleftharpoons \text{Zr}^{4+}$

In titanites of pegmatite ijolite from Las Montañetas substitutions b) and c) are the most significant while in the crystals from biotitic malignites of Playa del Águila mechanisms a) is the most important.

Figure S9 shows the chondrite-normalized composition of the analyzed titanites. They show a very flat spectrum. with a small Ce anomaly, typical of titanites from ultra-alkaline rocks [77]. In the zoned crystal from the biotitic malignites from La Playa del Águila, the REE contents increase from core to rim.

3.2.9. Apatite

Apatite $[\text{Ca}_5(\text{PO}_4)_3(\text{OH}, \text{F}, \text{Cl})]$ is an ubiquitous accessory. It occurs both as isolated ovoid crystals and as clusters of equigranular crystals located within discrete bands parallel to the foliation in deformed carbonatites. Some representative analyses are given in Table S9. Among the minor elements only SrO occurs in significant amounts, that suggests substitution mechanism $\text{Ca}^{2+} \rightleftharpoons \text{Sr}^{2+}$. Analyzed crystals are fluorapatites ss. $\text{Ca}_5(\text{PO}_4)_3\text{F}$. Low concentrations of Na_2O (up to 0.12 wt%) and SiO_2 (up to 0.68 wt%) suggest that belovite ($2\text{Ca}^{2+} \rightleftharpoons \text{Na}^+ + \text{REE}-\text{Y}^{3+}$) and britholite ($\text{Ca}^{2+} + \text{P}^{5+} \rightleftharpoons \text{REE}^{3+} + \text{Si}^{4+}$) substitutions are not significant (Figure S10).

Perovskite

Perovskite compositions from the ultra-alkaline Esquinzo Complex (Table S11) are perovskite s.s. (calcium titanate). Minor amounts of Na (up to 0.87 wt% Na_2O) and REE (up to 2.48 wt% Ce_2O_3) substitute for Ca and minor amounts of Nb (up to 1.03 wt%) and Fe (Fe_2O_3 up to 1.01 wt%) substitute for Ti, that suggests the following substitution mechanism (Table S11; Figure S11):

- 1). $2\text{Ca}^{2+} \rightleftharpoons (\text{Y}^{3+}, \text{REE}^{3+}) + \text{Na}^+$ (perovskite-loparite)
- 2). $2\text{Ti}^{4+} \rightleftharpoons \text{Nb}^{5+} + \text{Fe}^{3+}$ (perovskite-latrappite)

The importance of these two substitution mechanisms increases with magmatic differentiation from pyroxenites-melteigites to pegmatite ijolites from Las Montañetas.

The chondrite-normalized patterns of the crystals of the pegmatite ijolite from Las Montañetas (Figure S11) show significant REE fractionation.

Compared with perovskites from other carbonatite complexes, the Esquinzo perovskites fall within the compositional ranges for perovskites from Magnet Cove ijolites [78], from Oldoinyo Lengai jacupirangite and ijolite xenoliths [74] and from the Gardiner Complex melilitolite [79].

Pyrochlore

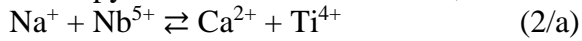
Pyrochlore in nepheline syenites-carbonatite composite dykes (silicocarbonatites) from Las Montañetas forms allotriomorphic or hypidiomorphic grains that are commonly fractured and occasionally zoned. Atomic proportions were calculated on the basis of $(\text{Nb} + \text{Ta} + \text{Ti}) = 2$ apfu (Table S12; Figure S12) [80, 81]. The crystals analyzed are fluorocalciopyrochlore and oxycalcipyrochlores, and show low Ta/Nb ratios typical of carbonatitic rocks (with Ta contents often below detection limit in the crystals analyzed [82, 83]). The A-site (Table S12) is mainly occupied by Ca and also by REE and only in some cases by Na and Sr. In some crystals, Th contents (0.12 a.p.f.u.) are high.

The composition of the pyrochlores analyzed can be explained by different substitution mechanisms (Table S12):

- 1) Coupled A–Y-site substitutions, as proposed by [84–86] to explain the high F contents observed in pyrochlore crystals (fluorocalciopyrochlores) found in some crystals
- $$\text{Na}^+ + \text{F}^- \rightleftharpoons \text{Ca}^{2+} + \text{O}^{2-} \quad (1/a)$$
- and
- $$\text{Na}^+ + \text{F}^- \rightleftharpoons \square^{\text{A}} + \square^{\text{Y}} \quad (1/b)$$

2) Coupled A–B-site substitutions (Figure S12, (Na+Nb) vs. (Ca+Ti) and (REE+Ti) vs. (Ca+Nb) plots):

Calciopyrochlore \rightleftharpoons Calciobetafite, $\text{NaCaNb}_2\text{O}_6(\text{OH}, \text{F}) \rightleftharpoons \text{Ca}_2\text{TiNbO}_6(\text{OH}, \text{F})$, i.e.

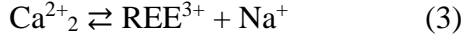


and $\text{NaCaNb}_2\text{O}_6(\text{OH}, \text{F}) \rightleftharpoons \text{REENaTiNbO}_6(\text{OH}, \text{F})$, i.e.



3) Pure A-site substitution (Figure S12, (Na+REE) vs. Ca diagram):

$\text{Ca}_2\text{NbO}_6(\text{OH}, \text{F}) \rightleftharpoons \text{REENaNbO}_6(\text{OH}, \text{F})$, i.e.



The chondrite-normalized REE patterns of pyrochlores of this study (Figure S12) exhibit a small enrichment in LREE and display a slight Ce positive anomaly. This positive cerium anomaly characterizes pyrochlore group minerals from carbonatite but also appears in pyrochlore and betafite from skarn deposits, fenite, nepheline syenite and aegirine syenite and is apparently structurally controlled [87].